Inorg. Chem. **2005**, *44*, 8510–8520

Disilver(I) Rectangular-Shaped Metallacycles: X-ray Crystal Structure and Dynamic Behavior in Solution

Chun-Long Chen,[†] Hai-Yan Tan,[†] Jun-Hua Yao,[†] Yi-Qian Wan,[†] and Cheng-Yong Su*[,†,‡]

State Key Laboratory of Optoelectronic Materials and Technologies, School of Chemistry and Chemical Engineering and Instrumentation Analysis & Research Center, Sun Yat-Sen University, Guangzhou 510275, China, and The State Key Laboratory of Structural Chemistry, Fujian Institute of Research on the Structure of Matter, Chinese Academy of Sciences, Fuzhou 350002, China

Received May 1, 2005

Reaction of the ditopic semirigid ligand 1,2-bis(imidazolylmethyl)benzene (1,2-bImb) or the flexible ligand 1,4-bis-(2-benzimidazolyl)butane (C4BIm) with AgX (X = ClO_4^-, BF_4^-, $CF_3CO_2^-$) afforded five new complexes, namely, $[Ag_2(1,2\text{-bImb})_2](ClO_4)_2$ (**1**), $[Ag_2(1,2\text{-bImb})_2](BF_4)_2$ (**2**), $[Ag_2(1,2\text{-bImb})_2](CF_3CO_2)_2\cdot 2CH_3OH$ (**3**·2CH_3OH), $[Ag_2(C4BIm)_2]$-$(ClO_4)_2\cdot$2DMF (**4**·2DMF), and $[Ag_2(C4BIm)_2](CF_3CO_2)_2\cdot 2H_2O$ (**5**·2H_2O), all of which contain a centrosymmetric, rectangular-shaped cationic disilver(I) metallacycle $[Ag_2(L)_2]^{2+}$. In **1**–**3**, a pair of 1,2-bImb ligands takes on the syn conformation to connect two Ag(I) ions to give a compressed rectangle with a transannular Ag···Ag separation of 3.27–3.36 Å, whereas in **4** and **5**, the pair of planar C4BIm ligands acts in the cis conformation to connect two Ag(I) ions to yield a normal rectangle with a transannular Ag···Ag separation of 7.67–7.91 Å. The anions form Ag···O or Ag···F weak interactions in **1**–**3** and O–H···O or N–H···O hydrogen bonds in **4** and **5** in crystal packing but exhibit no significant influence on the formation of the disilver(I) macrocycles. The solution structure and dynamic behavior of the complexes studied by electrospray ionization mass spectrometry, ^{1}H NMR, and variable-temperature NMR indicated that the dynamic equilibrium between the $[Ag_2(L)_2]^{2+}$ cation and the open-ring oligomers or other potential species occurs via solvent-assisted dissociative exchange. The metal–ligand exchange barrier was estimated to be 54.5 kJ mol^{-1}.

Introduction

The programmed self-assembly of discrete molecular architectures, such as coordination polyhedral cages and polygonal macrocycles, has been the subject of extensive studies over the past decade because of their potential applications in molecular recognition, separation, and storage.[1] The most common approach to synthesize such compounds is to combine organic ligands favoring structure-specific self-assembly with various coordination centers provided by the plethora of metal ions. This strategy has proved to be effective for the organization of molecular polygons.[2,3] In contrast, the construction of relatively simple rectangular-shaped molecules with low symmetry presents difficulties, mainly because a combination of metal ions with two kinds of organic ligands of different length tends to give a mixture of small and large squares rather than a rectangle. We recently proposed a *ligand-directed* construction ap-

* To whom correspondence should be addressed. E-mail: cedc63@zsu.edu.cn.

† Sun Yat-Sen University.

‡ Chinese Academy of Sciences.

(1) (a) Swiegers, G. F.; Malefetse, T. J. *Chem. Rev.* **2000**, *100*, 3483. (b) Saalfrank, R. W.; Uller, E.; Demleitner, B.; Bernt, I. *Struct. Bonding* **2000**, *96*, 149. (c) Caulder, D. L.; Raymond, K. N. *Acc. Chem. Res.* **1999**, *32*, 975. (d) Morgan, M.; Rebek, J., Jr. *Chem. Rev.* **1997**, *97*, 1647. (e) Jones, C. J. *Chem. Soc. Rev.* **1998**, *27*, 289. (f) Fujita, M. *Chem. Soc. Rev.* **1998**, *27*, 417. (g) Jacopozzi, P.; Dalcanale, E. *Angew. Chem., Int. Ed. Engl*. **1997**, *36*, 613. (h) Albrecht, M.; Röttele, H.; Burger, P. *Chem.—Eur. J.* **1996**, *2*, 1264. (i) Leininger, S.; Olenyuk, B.; Stang, P. J. *Chem. Rev.* **2000**, *100*, 853.

(2) (a) Steel, P. J.; Sumby, C. J. *Chem. Commun.* **2002**, 322. (b) Caradoc-Davies, P. L.; Hanton, L. R. *J. Chem. Soc., Dalton Trans.* **2003**, 1754. (c) Shin, D. M.; Lee, I. S.; Lee, Y.-A.; Chung, Y. K. *Inorg. Chem.* **2003**, *42*, 2977. (d) Navarro, J. A. R.; Lippert, B. *Coord. Chem. Rev.* **2001**, *222*, 219. (e) Su, C.-Y.; Cai, Y.-P.; Chen, C.-L.; Zhang, H.-X.; Kang, B.-S. *J. Chem. Soc., Dalton Trans.* **2001**, 359. (f) Su, C.-Y.; Cai, Y.-P.; Chen, C.-L.; Lissner, F.; Kang, B.-S.; Kaim, W. *Angew. Chem., Int. Ed.* **2002**, *41*, 3371. (g) He, C.; Wang, L.-Y.; Wang, Z.-M.; Liu, Y.; Liao, C.-S.; Yan, C.-H. *J. Chem. Soc., Dalton Trans.* **2002**, 134. (h) Dinolfo, P. H.; Williams, M. E.; Stern, C. L.; Hupp, J. T. *J. Am. Chem. Soc.* **2004**, *126*, 12989. (i) Thanasekaran, P.; Liao, R.-T.; Liu, Y.-H.; Rajendran, T.; Rajagopal, S.; Lu, K.-L. *Coord. Chem. Rev.* **2005**, *249*, 1085.

10.1021/ic050673o CCC: $30.25
Published on Web 10/20/2005

proach by designing organic molecular clips that provide two parallel coordination sites facing the same direction and achieved spontaneous assembly of molecular rectangles and prismatic cages.[4] This may be an alternative approach with respect to Stang's clips by avoiding the predesign of organometallic precursors.[5]

Because our previous approach made use of rigid or semirigid ligands, we are interested in extending it to flexible ligands bearing similar "clip" characteristics. Construction of discrete molecular structures with flexible ligands is far less common in comparison to the conformationally rigid ligands because of the less predictable assembly process.[6] However, the incorporation of flexible components may endow the molecular architectures with potential advantages: for example, a "breathing" ability in the solid state and adaptive recognition properties as a function of coexisting guests or counterions.[7] On the other hand, the flexibility of the ligand leads to the formation of both discrete macrocycles and infinite polymeric structures on the basis of the conformational freedom of the connecting fragment.[8] In most cases, the coordination polymers can be crystallized, but little attention has been paid to their assembly mechanism in solution. Our group and others[2c,9] recently reported the interesting conversion of discrete coordination assemblies to polymeric structures, and the formation of infinite polymers from ring-opening isomerization of closed cyclic or cage precursors has been speculated. This prompted us to conduct an investigation of the solution structure and dynamics, hoping to gain some insight into the general mechanism of self-assembly and the relationship between the closed and extended structures.

The solution dynamics behavior monitored by NMR and mass spectrometry (MS) techniques has been vigorously explored in various self-assembled supramolecular systems,[10,11] where variable-temperature NMR (VT-NMR) represents a useful tool to elucidate structural conversions such as enantiomerization,[12] conformational and linkage isomerization,[13] and ligand exchange or equilibrium.[14] Silver(I) complexes are known to be labile in solution, and rapid exchange may occur on the NMR time scale at ambient temperature.[15] Although solution dynamics investigations have been well carried out for several silver(I)−nitrogen donor systems,[2f,4,15,16] further work is warranted in view of the large assortment of Ag(I) coordination assemblies constructed hitherto. We have previously reported a series of discrete silver(I) molecular architectures[2f,4] and their solution dynamics behavior. In this paper, we report five

(3) (a) Beauchamp, D. A.; Loeb, S. J. *Chem. Commun.* **2002**, 2484. (b) Liu, G.-F.; Ye, B.-H.; Ling, Y.-H.; Chen, X.-M. *Chem. Commun.* **2002**, 1442. (c) Zhao, Y. J.; Hong, M. C.; Sun, W. P.; Cao, R.; Zhou, Z. Y.; Chan, A. S. C. *Chem. Lett.* **2002**, 28. (d) Cui, Y.; Ngo, H. L.; Lin, W. B. *Inorg. Chem.* **2002**, *41*, 1033. (e) Ruben, M.; Lehn, J.-M.; Vaughan, G. *Chem. Commun.* **2003**, 1338. (f) Khlobystov, A. N.; Brett, M. T.; Blake, A. J.; Champness, N. R.; Gill, P. M. W.; O'Neill, D. P.; Teat, S. J.; Wilson, C.; Schröder, M. *J. Am. Chem. Soc.* **2003**, *125*, 6753. (g) Zheng, S. L.; Zhang, J.-P.; Wong, W.-T.; Chen, X.-M. *J. Am. Chem. Soc.* **2003**, *125*, 6882.

(4) (a) Su, C.-Y.; Cai, Y.-P.; Chen, C.-L.; Smith, M. D.; Kaim, W.; zur Loye, H.-C. *J. Am. Chem. Soc.* **2003**, *125*, 8595. (b) Cai, Y.-P.; Su, C.-Y.; Zhang, H.-X.; Zhou, Z.-Y.; Zhu, L.-X.; Chan, A. S. C.; Liu, H.-Q.; Kang, B.-S. *Z. Anorg. Allg. Chem.* **2002**, *628*, 2321.

(5) (a) Kuehl, C. J.; Huang, S. D.; Stang, P. J. *J. Am. Chem. Soc.* **2001**, *123*, 9634. (b) Kuehl, C. J.; Yamamoto, T.; Seidel, S. R.; Stang, P. J. *Org. Lett.* **2002**, *4*, 913. (c) Caskey, D. C.; Shoemaker, R. K.; Michl, J. *Org. Lett.* **2004**, *6*, 2039.

(6) (a) Tabellion, F. M.; Seidel, S. R.; Arif, A. M.; Stang, P. J. *J. Am. Chem. Soc.* **2001**, *123*, 7740. (b) Tabellion, F. M.; Seidel, S. R.; Arif, A. M.; Stang, P. J. *J. Am. Chem. Soc.* **2001**, *123*, 11982. (c) Fujita, M.; Ibukuro, F.; Ogura, K.; Seki, H.; Kamo, O.; Imanari, M. *J. Am. Chem. Soc.* **1996**, *118*, 899.

(7) (a) Chatterjee, B.; Noveron, J. C.; Resendiz, M. J. E.; Liu, J.; Yamamoto, T.; Parker, D.; Cinke, M.; Nguyen, C. V.; Arif, A. M.; Stang, P. J. *J. Am. Chem. Soc.* **2004**, *126*, 10654. (b) Yue, N. L. S.; Jennings, M. C.; Puddephatt, R. J. *Inorg. Chem.* **2005**, *44*, 1125. (c) Raehm, L.; Mimassi, L.; Guyard-Duhayon, C.; Amouri, H. *Inorg. Chem.* **2003**, *42*, 5654.

(8) (a) Cai, Y.-P.; Zhang, H.-X.; Xu, A.-W.; Su, C.-Y.; Chen, C.-L.; Liu, H.-Q.; Zhang, L.; Kang, B.-S. *J. Chem. Soc., Dalton Trans.* **2001**, 2429. (b) Chen, C.-L.; Su, C.-Y.; Cai, Y.-P.; Zhang, H.-X.; Xu, A.-W.; Kang, B.-S.; zur Loye, H.-C. *Inorg. Chem.* **2003**, *42*, 3738. (c) Xu, A.-W.; Cai, Y.-P.; Shi, J.-L.; Tong, Y.-X.; Su, C.-Y.; Kang, B.-S. *Chin. J. Struct. Chem.* **2002**, *21*, 683. (d) Muthu, S.; Yip, J. K. K.; Vittal, J. J. *J. Chem. Soc., Dalton Trans.* **2001**, 3577. (e) Muthu, S.; Yip, J. H. K.; Vittal, J. J. *J. Chem. Soc., Dalton Trans.* **2002**, 4561. (f) Zou, R.-Q.; Li, J.-R.; Xie, Y.-B.; Zhang, R.-H.; Bu, X.-H. *Cryst. Growth Des.* **2004**, *4*, 79. (g) Xie, Y.-B.; Zhang, C.; Li, J.-R.; Bu, X.-H. *J. Chem. Soc., Dalton Trans.* **2004**, 562. (h) Bu, X.-H.; Chen, W.; Hou, W.-F.; Du, M.; Zhang, R.-H.; Brisse, F. *Inorg. Chem.* **2002**, *41*, 3477.

(9) (a) Su, C.-Y.; Goforth, A. M.; Smith, M. D.; zur Loye, H.-C. *Inorg. Chem.* **2003**, *42*, 5685. (b) Miller, P.; Nieuwenhuyzen, M.; Charman, J. P. H.; James, S. L. *CrsytEngComm* **2004**, *6*, 408. (c) Lozano, E.; Nieuwenhuyzen, M.; James, S. L. *Chem.—Eur. J.* **2001**, *7*, 2644. (d) Qin, Z.; Jennings, M. C.; Puddephatt, R. J. *Chem.—Eur. J.* **2002**, *8*, 735.

(10) (a) Hori, A.; Yamashita, K.-i.; Kusukawa, T.; Akasaka, A.; Biradha, K.; Fujita, M. *Chem. Commun.* **2004**, 1798. (b) Hori, A.; Yamashita, K.-i.; Fujita, M. *Angew. Chem., Int. Ed.* **2004**, *43*, 5016. (c) Krupenya, D. V.; Selivanov, S. I.; Tunik, S. P.; Haukka, M.; Pakkanen, T. A. *Dalton Trans.* **2004**, 2541. (d) Jia, W.-L.; Wang, R.-Y.; Song, D. T.; Ball, S. J.; McLean, A. B.; Wang, S. *Chem.—Eur. J.* **2005**, *11*, 832. (d) Jodry, J. J.; Lacour, J. *Chem.—Eur. J.* **2000**, *6*, 4297.

(11) (a) Hiraoka, S.; Hirata, K.; Shionoya, M. *Angew. Chem., Int. Ed.* **2004**, *43*, 3814. (b) Wolf, R.; Hey-Hawkins, E. *Chem. Commun.* **2004**, 2626. (c) Cragg, P. J.; Heirtzler, F. R.; Howard, M. J.; Prokes, I.; Weyhermüller, T. *Chem. Commun.* **2004**, 280. (d) Childs, L. J.; Pascu, M.; Clarke, A. J.; Alcock, N. W.; Hannon, M. J. *Chem.—Eur. J.* **2004**, *10*, 4291. (e) Gao, H. Y.; Guo, W. J.; Bao, F.; Gui, G. Q.; Zhang, J. K.; Zhu, F. M.; Wu, Q. *Organometallics* **2004**, *23*, 6273. (f) Burchell, T. J.; Eisler, D. J.; Jennings, M. C.; Puddephatt, R. J. *Chem. Commun.* **2003**, 2228. (g) Santra, B. K.; Liaw, B.-J.; Hung, C.-M.; Liu, C. W. *Inorg. Chem.* **2003**, *42*, 8866. (h) Niu, W. J.; Wong, E. H.; Weisman, G. R.; Peng, Y. J.; Anderson, C. J.; Zakharov, L. N.; Golen, J. A.; Rheingold, A. L. *Eur. J. Inorg. Chem.* **2004**, 3310. (i) Demšar, A.; Košmrlj, J.; Petriček, S. *J. Am. Chem. Soc.* **2002**, *124*, 3951.

(12) (a) Saalfrank, R. W.; Demleitner, B.; Glaser, H.; Maid, H.; Bathelt, D.; Hampel, F.; Bauer, W.; Teichert, M. *Chem.—Eur. J.* **2002**, *8*, 2679. (b) Desvergnes-Breuil, V.; Hebbe, V.; Dietrich-Buchecker, C.; Sauvage, J.-P.; Lacour, J. *Inorg. Chem.* **2003**, *42*, 255. (c) Olenyuk, B.; Whiteford, J. A.; Stang, P. J. *J. Am. Chem. Soc.* **1996**, *118*, 8221.

(13) (a) Harman, W. D. *Chem. Coord. Rev.* **2004**, *248*, 853. (b) Harman, W. D.; Sekine, M.; Taube, H. *J. Am. Chem. Soc.* **1988**, *110*, 5725. (c) Reich, H. J.; Goldenberg, W. S.; Gudmundsson, B. Ö.; Sanders, A. W.; Kulicke, K. L.; Simon, K.; Guzei, I. A. *J. Am. Chem. Soc.* **2001**, *123*, 8067.

(14) (a) Hiraoka, S.; Shiro, M.; Shionoya, M. *J. Am. Chem. Soc.* **2004**, *126*, 1214. (b) Riesgo, E.; Hu, Y.-Z.; Bouvier, F.; Thummel, R. P. *Inorg. Chem.* **2001**, *40*, 2541. (c) Park, S. J.; Shin, D. M.; Sakamoto, S.; Yamaguchi, K.; Chung, Y. K.; Lah, M. S.; Hong, J.-I. *Chem.—Eur. J.* **2005**, *11*, 235. (d) Kajiwara, T.; Yokozawa, S.; Ito, T.; Iki, N.; Morohashi, N.; Miyano, S. *Angew. Chem., Int. Ed.* **2002**, *41*, 2076.

(15) (a) Provent, C.; Rivara-Minten, E.; Hewage, S.; Brunner, G.; Williams, A. F. *Chem.—Eur. J.* **1999**, *5*, 3487. (b) Carina, R. F.; Williams, A. F.; Piguet, C. *Helv. Chim. Acta* **1998**, *81*, 548. (c) Marquis, A.; Kintzinger, J.-P.; Graff, R.; Baxter, P. N. W.; Lehn, J.-M. *Angew. Chem., Int. Ed.* **2002**, *41*, 2760. (d) Barboiu, M.; Vaughan, G.; Kyritsakas, N.; Lehn, J.-M. *Chem.—Eur. J.* **2003**, *9*, 763. (e) Eisler, D. J.; Kirby, C. W.; Puddephatt, R. J. *Inorg. Chem.* **2003**, *42*, 7626.

(16) (a) Hiraoka, S.; Yi, T.; Shiro, M.; Shionoya, M. *J. Am. Chem. Soc.* **2002**, *124*, 14510. (b) Hiraoka, S.; Harano, K.; Tanaka, T.; Shiro, M.; Shionoya, M. *Angew. Chem., Int. Ed.* **2003**, *42*, 5182.

Scheme 1. Preparation of Ligands and Their Ag(I) Complexes

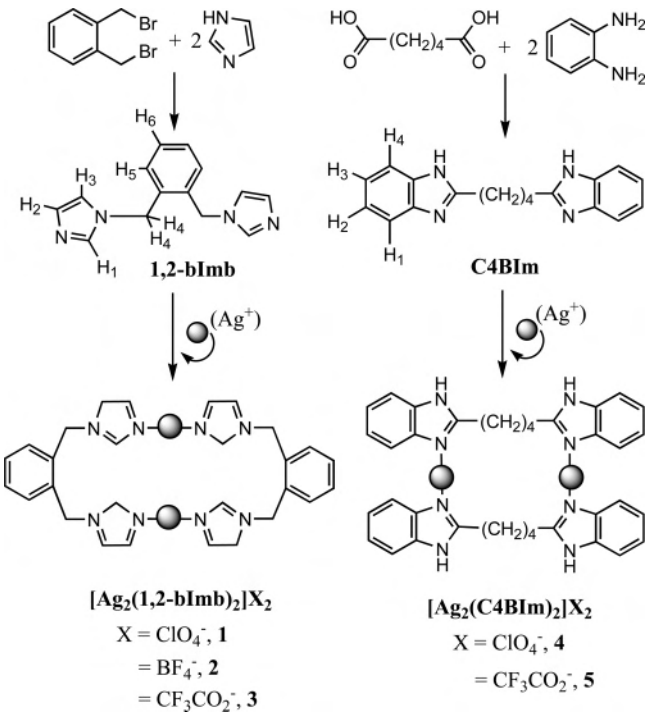

disilver(I) metallacyclic structures synthesized using a semirigid ligand, 1,2-bis(imidazolylmethyl)benzene (1,2-bImb), and a flexible ligand, 4,4′-bis(2-benzimidazolyl)butane (C4BIm), namely, $[Ag_2(1,2\text{-bImb})_2](ClO_4)_2$ (**1**), $[Ag_2(1,2\text{-bImb})_2](BF_4)_2$ (**2**), $[Ag_2(1,2\text{-bImb})_2](CF_3CO_2)_2\cdot 2CH_3OH$ (**3**·$2CH_3OH$), $[Ag_2(C4BIm)_2](ClO_4)_2\cdot 2DMF$ (**4**·2DMF), and $[Ag_2(C4BIm)_2](CF_3CO_2)_2\cdot 2H_2O$ (**5**·$2H_2O$). Complexes **1**−**3** provide a feasible model to acquire solution structure information via ^1H NMR and electrospray ionization MS (ESI-MS) measurements, while **4** and **5** can be used to explore the dynamic equilibrium of solution species by variable-temperature ^1H NMR. Different anions were selected to explore the effect of their coordination ability, size, and shape on the resulting structures.

Results and Discussion

Synthesis and Characterization. Two structurally related ligands, flexible C4BIm and semiflexible 1,2-bImb, have been employed to synthesize disilver(I) complexes **1**−**5**. The ligand C4BIm contains the aliphatic $(CH_2)_4$ backbone with two 2-benzimidazolyl (BIm) rings acting as terminal coordinating groups, while the ligand 1,2-bImb consists of the rigid *o*-xylylene spacer and two 1-imidazolyl (Im) rings. Scheme 1 illustrates the synthetic procedure of the two ligands and their reaction with silver salts AgX ($X = ClO_4^-$, $CF_3CO_2^-$, or BF_4^-). It was found that altering the anions of various shapes and coordinating ability did not affect the formation of binuclear $[Ag_2L_2]^{2+}$ cations but showed a slight influence on their cavity size[7b] and a remarkable influence on their packing in the solid sate (vide post).

The infrared spectra of complexes **1**−**3** all exhibit characteristic absorptions for ligand 1,2-bImb with a slight shift due to coordination. In complex **1**, the absorption bands appearing at 1085 (ν_3) and 623 cm^{-1} (ν_4) are characteristic of a noncoordinated perchlorate ion.[17] The absorption band at 1076 cm^{-1} indicates the existence of the BF_4^- anion in complex **2**. The strong absorption bands at 1685 and 1459 cm^{-1} in complex **3** are assigned to ν_{as} and ν_s vibrations of the $CF_3CO_2^-$ anion,[18] respectively. The IR spectra of complexes **4** and **5** feature basically C4BIm ligand absorptions. The characteristic bands of the "free" perchlorate ion in **4** appear at 1089 (ν_3) and 621 cm^{-1} (ν_4). The absorption band at 1659 cm^{-1} occurs as a result of the stretching vibration $\nu_{C=O}$ of solvated DMF molecules, which is slightly red-shifted compared to that of "free" DMF,[19] probably owing to the formation of N−H···O hydrogen bonds with C4BIm. The broad band centered at 3280 cm^{-1} in **4** can be assigned to ν_{N-H} of the C4BIm ligand, and the broadness is indicative of hydrogen bonding in accordance with the crystal structural analysis. In complex **5**, the ν_{as} and ν_s bands of the $CF_3CO_2^-$ anion appear at 1674 and 1454 cm^{-1}, respectively. The solvated water molecule in **5** shows a broad band at 3310−3450 cm^{-1}, which overlaps with the NH absorption.

Crystal Structure. The crystallographic analyses of complexes **1**−**3** showed that they are all composed of a dimeric cation $[Ag_2(1,2\text{-bImb})_2]^{2+}$, which weakly interacts with two counteranions, as depicted in Figure 1. Because of the semiflexibility arising from the methylene groups ($-CH_2-$), two imidazolyl arms of each ligand adopt the syn conformation, with the two imidazole rings nearly parallel to each other (dihedral angles: 15.26° for **1**, 15.53° for **2**, and 17.57° for **3**). Thus, two Ag(I) ions join two 1,2-bImb ligands to result in a "compressed" rectangular-shaped macrocycle containing intramolecular $\pi\cdots\pi$ interactions (centroid-to-centroid distances: 3.494 Å for **1**, 3.491 Å for **2**, and 3.527 Å for **3**). The metallacycle exhibits an overall chairlike conformation possessing a crystallographically imposed inversion center. Each silver(I) ion is coordinated to two imidazole N donors, with the N−Ag−N bond angles close to linearity (see Table 2). Two diametrically positioned anions weakly bridge the two Ag(I) ions in a bidentate manner [Ag(A)···O(3) 2.899 Å and Ag···O(2) 2.992 Å in **1**; Ag(A)···F(4) 2. 964 Å and Ag···F(3) 2.959 Å in **2**; and Ag(A)···O(2) 2.696 Å and Ag···O(1) 2.953 Å in **3**]. Although the BF_4^- anions in **2** are slightly disordered, the bridging fluorine atoms are well located. The short transannular Ag···Ag separations (3.339 Å in **1**, 3.364 Å in **2**, and 3.271 Å in **3**) in these dimeric cations are comparable with the sum of the van der Waals radii of two silver atoms (3.440 Å),[20] precluding any effective space inside the metallacycles.[7b] Therefore, formation of such compressed metallacycles may be attributed to the synergistic effects involving intramolecular $\pi\cdots\pi$ stacking, weak Ag···Ag interactions, and

(17) (a) Su, C.-Y.; Kang, B.-S.; Du, C.-X.; Yang, Q.-C.; Mak, T. C. W. *Inorg. Chem.* **2000**, *39*, 4843. (b) Agarwal, R. K.; Sarin, R. K. *Polyhedron* **1993**, *19*, 2411. (c) Pettinari, C.; Marchetti, F.; Polimante, R.; Cingolani, A.; Portalone, G.; Colapietro, M. *Inorg. Chim. Acta* **1996**, *249*, 215.
(18) (a) Wojtczak, W. A.; Hampden-Smith, M. J.; Duesler, E. N. *Inorg. Chem*. **1998**, *37*, 1781. (b) Harrison, P. G.; Guest, A. *J. Chem. Soc., Faraday Trans.* **1991**, *87*, 1929.
(19) Moghimi, A.; Alizadeh, R.; Shokrollahi, A.; Aghabozorg, H.; Shamsipur, M.; Shochravi, A. *Inorg. Chem*. **2003**, *42*, 1616.
(20) Bondi, A. *J. Phys. Chem*. **1994**, *68*, 441.

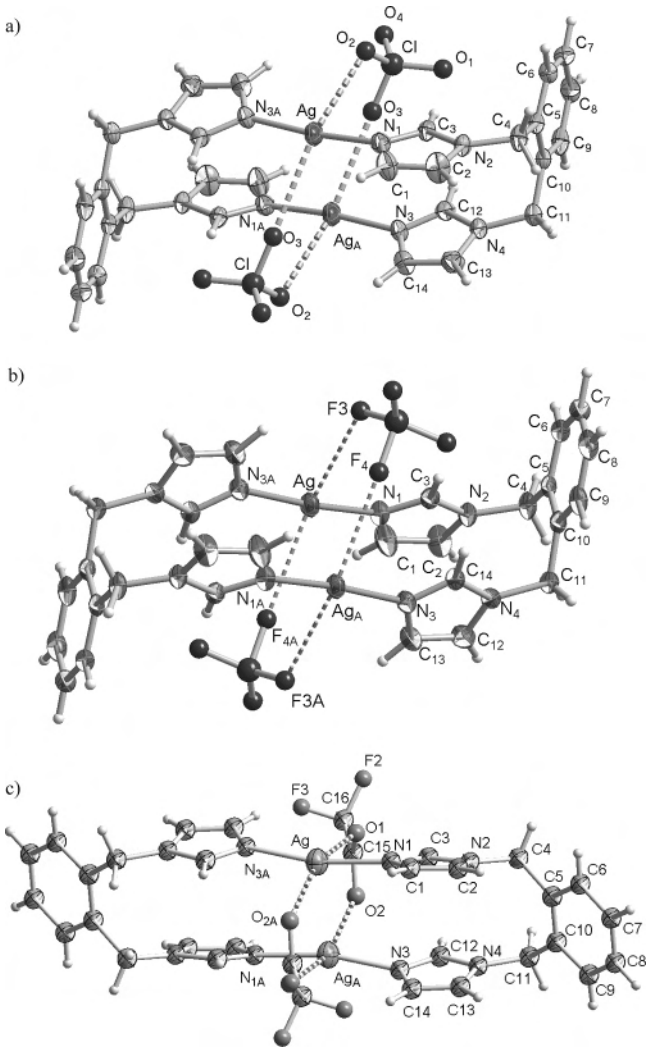

Figure 1. View of the cationic metallacycles $[Ag_2(1,2\text{-bimb})_2]^{2+}$ clamped by weakly interacted anions in (a) **1**, (b) **2**, and (c) **3**. Displacement ellipsoids drawn at the 50% probability level with anions in a ball-and-stick mode. Symmetry code: (A) $-x + 1, -y + 2, -z + 1$.

clamping of silver(I) ions by anions. Two solvated CH_3OH molecules in **3** form O−H···O hydrogen bonds (O···O 2.751 Å) with the oxygen atoms of $CF_3CO_2^-$.

X-ray crystal structure analyses confirmed that complexes **4** and **5** consist of a centrosymmetric dimeric cation $[Ag_2(C4BIm)_2]^{2+}$, two noncoordinated anions, and two solvated molecules, as depicted in Figure 2, with each C4BIm ligand acting in the ditopic bis(monodentate) mode. Each silver atom is almost linearly coordinated by two ligands [N−Ag−N 170.09(11)° (**4**) and 176.28(11)° (**5**)], and the two BIm arms of each ligand adopt the cis conformation such that the macrocycles in **4** and **5** are nearly coplanar. The mean deviations of the plane including all non-H atoms of the cation are 0.0784 Å for **4** and 0.4061 Å for **5**. Therefore, the dimeric $[Ag_2(C4BIm)_2]^{2+}$ cations exhibit the normal rectangular shape, which is significantly different from the "compressed" one in **1**−**3**. The transannular Ag···Ag separations (7.669 Å in **4** and 7.906 Å in **5**) are more than twice as long as those in **1**−**3**, excluding the formation of intramolecular $\pi\cdots\pi$ stacking and Ag···Ag interactions. In contrast to those in **1**−**3**, both the weakly coordinating

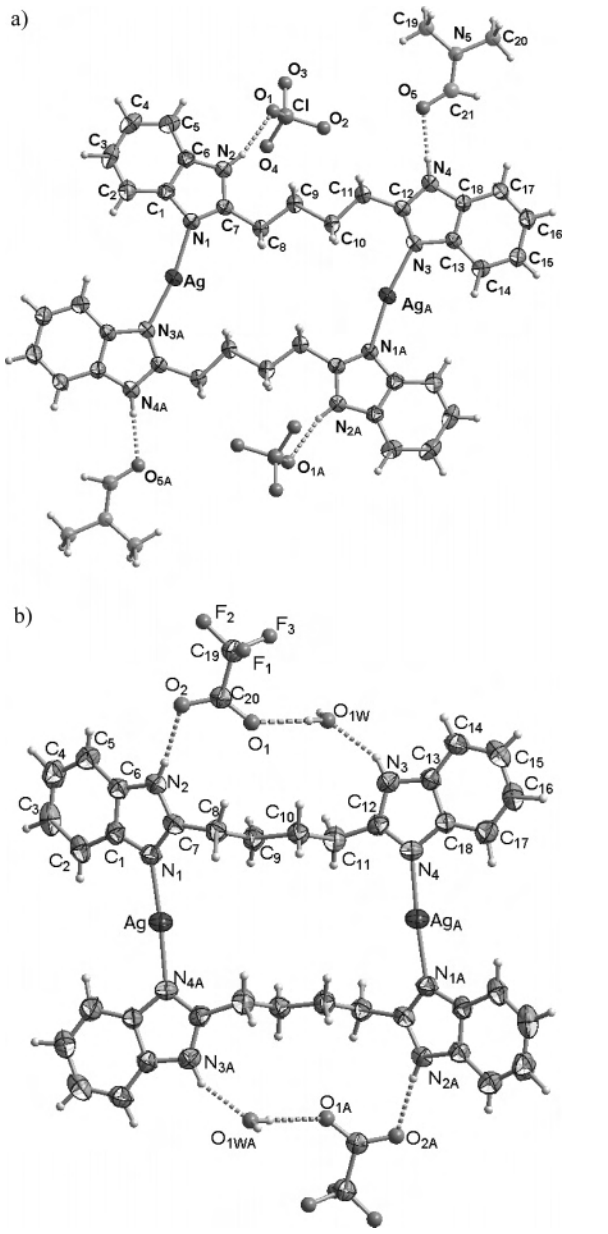

Figure 2. View of the cationic metallacycles $[Ag_2(C4Bim)_2]^{2+}$ showing hydrogen-bonded anions and solvated molecules in (a) **4**·2DMF and (b) **5**·$2H_2O$. Displacement ellipsoids drawn at the 50% probability level with anions in a ball-and-stick mode. Symmetry codes: **4**·2DMF, (A) $-x + 1, -y + 1, -z + 2$; **5**·$2H_2O$, (A) $-x, -y, -z$.

$CF_3CO_2^-$ and noncoordinating ClO_4^- anions do not form Ag···O interactions to "clamp" two Ag(I) ions. Alternatively, each dimeric cation forms four hydrogen bonds with the two counteranions and two solvated molecules via the NH groups of the BIm rings. In **5**, the hydrogen-bonded $[Ag_2(C4BIm)_2]^{2+}$ cation, $CF_3CO_2^-$ anion, and solvated water further constitute two three-component rings on both sides of the metallacycle (Figure 2).

Crystal Packing. As one of important types of supramolecular forces, $\pi\cdots\pi$ stacking shows a specific structural requirement for substrate recognition or the arrangement of complicated architectures.[21] In complex **1** (or **2**), two types of intermolecular $\pi\cdots\pi$ stacking are present, as shown in Figure 3a, besides the intramolecular $\pi\cdots\pi$ interactions mentioned above. One is formed between phenyl rings

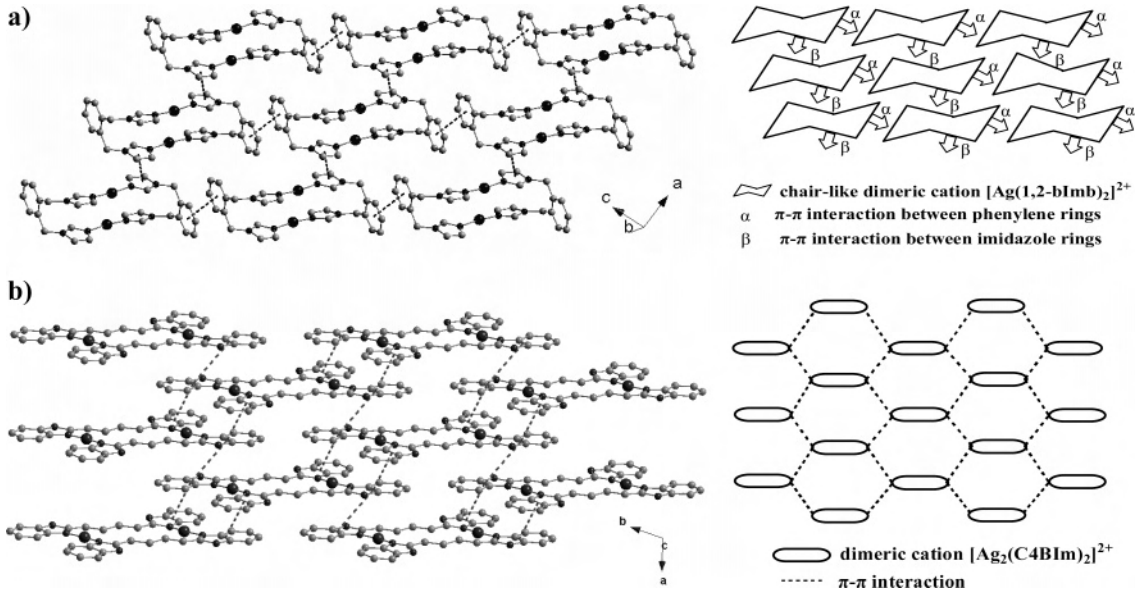

Figure 3. $\pi\cdots\pi$ stacking (indicated by dashed lines) and its schematic view in **1** (a) and **4** (b).

(labeled α, centroid-to-centroid distances: 3.750 Å in **1** and 3.752 Å in **2**) and the other between imidazolyl rings (labeled β, centroid-to-centroid distances: 3.640 Å in **1** and 3.720 Å in **2**). The α-type $\pi\cdots\pi$ interactions link the dimeric $[Ag_2L_2]^{2+}$ cations in an offset way to give an infinite 1D chain. Such chains are further recognized via the staggered β-type $\pi\cdots\pi$ interactions to result in a 2D layer in the *ac* plane, as shown in Figures 3a and S2a in the Supporting Information. The molecules are stacked up in these layers, leaving a large space in between to accommodate the counteranions (ClO_4^- or BF_4^-) as demonstrated in Figures S1 and S2b in the Supporting Information. By contrast, complex **3** shows only the α type of intermolecular $\pi\cdots\pi$ interactions, which join the dimeric $[Ag_2L_2]^{2+}$ cations into a 1D chain, as shown in Figure S3a in the Supporting Information. The β-type interactions are absent probably because of the existence of the solvated CH_3OH molecules, which form C−H···O hydrogen bonds (O···O 2.483 Å) with the anions (Figure S3a in the Supporting Information). However, the layered crystal packing mode is still maintained, with the $[Ag_2L_2]^{2+}$ cationic layer and the $CF_3CO_2^-$ and CH_3OH anionic layer alternately stacking up as shown in Figure S3b in the Supporting Information.

The rectangular $[Ag_2L_2]^{2+}$ cations in complex **4** stack up in an offset way with the formation of $\pi\cdots\pi$ interactions between BIm units (centroid-to-centroid distances: 3.718 and 3.896 Å), thus generating a 2D layer, which is shown in Figure 3b. Each dimeric cation overlaps with four neighboring cations in a manner similar to bricks in a masonry wall. Furthermore, the hydrogen bonds are formed between the cations and ClO_4^- anions and DMF molecules (N···O 2.704−2.955 Å and ∠NHO 153−175°; Figure S4a in the Supporting Information), which make the counteranions and solvated molecules interbedded between $[Ag_2L_2]^{2+}$ cationic layers, as depicted in Figure S4b in the Supporting Information. The $\pi\cdots\pi$ interactions between BIm units (centroid-to-centroid distances: 3.725 and 4.131 Å) in complex **5** also link the dimeric cations into a 2D brick layer (Figure S5a in the Supporting Information). More interestingly, two solvated H_2O molecules and two $CF_3CO_2^-$ anions form a hydrogen-bonded cyclic motif (O···O 2.784−2.892 Å and ∠OHO 153−173°), which connects the dimeric cations via N−H···O hydrogen bonds (N···O 2.724−2.788 Å and ∠NHO 153−175°) into a 1D chain, as shown in Figure S5b in the Supporting Information. The combination of $\pi\cdots\pi$ interactions and hydrogen bonds generates a 3D framework (Figure S5c in the Supporting Information) with counteranions and water molecules located between the layers of the metallacycles, as shown in Figure S5d in the Supporting Information.

Solution Structure and Dynamics. At room temperature, the ^{1}H NMR spectra of all complexes generally show a simple pattern containing one set of signals, indicative of either the formation of one single species in solution or the presence of rapid equilibration between exchanging species. Compared to the spectra of the "free" ligands, the proton signals of the complexes are shifted (downfield or upfield) and broadened to varied extents. This supports the second postulation due to the labile nature of the silver(I) complexes in solution as observed in related systems.[4,15,16,22,23] The questions then arise as to the nature and structure of the main species in solution.

Figure 4 displays the ^{1}H NMR spectra of 1,2-bImb and its complexes recorded in CD_3CN or DMSO-d_6 at room temperature. The proton resonance assignments have been confirmed by the 2D H,H−COSY spectrum of 1,2-bImb, where correlations between H_2 and H_3 and between H_5 and H_6 are evident, as shown in Figure S6 in the Supporting

(21) (a) Ponzini, F.; Zagha, R.; Hardcastle, K.; Siegel, J. S. *Angew. Chem., Int. Ed.* **2000**, *39*, 2323. (b) Fyfe, M. C. T.; Stoddart, J. F. *Acc. Chem. Res.* **1997**, *10*, 3393. (c) Janiak, C. *J. Chem. Soc., Dalton Trans.* **2000**, 3885 and references cited therein. (d) Ma, J. C.; Dougherty, D. A. *Chem. Rev.* **1997**, *97*, 1303.

(22) Caulder, D. L.; Powers, R. E.; Parac, T. N.; Raymond, K. N. *Angew. Chem., Int. Ed.* **1998**, *37*, 1840.

(23) Levin, M. D.; Stang, P. J. *J. Am. Chem. Soc.* **2000**, *122*, 7428.

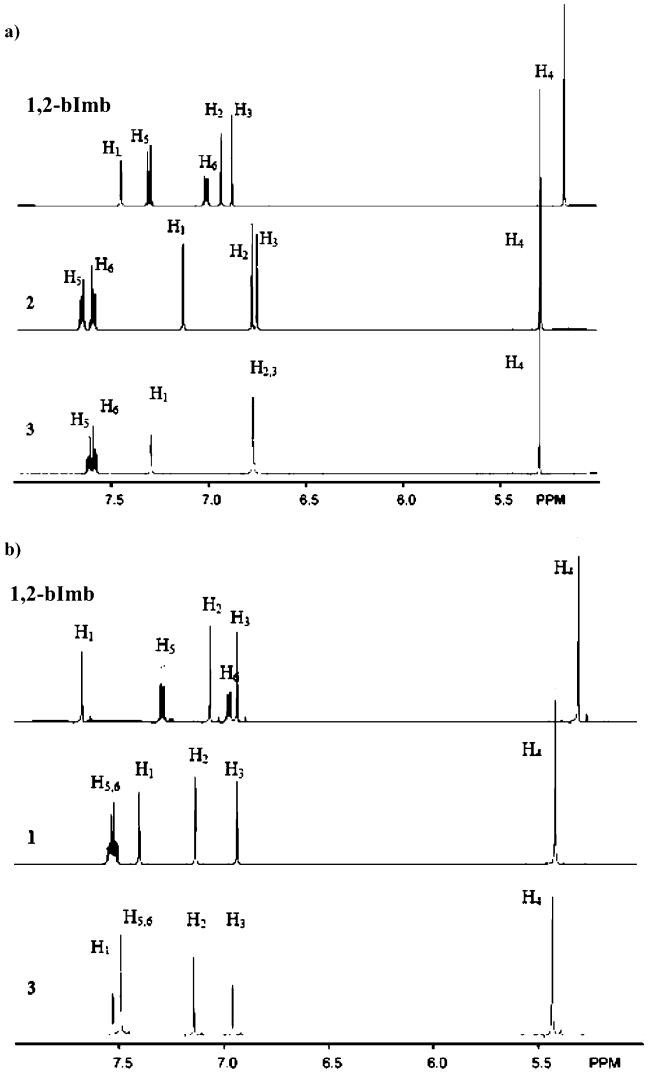

Figure 4. Partial ^{1}H NMR spectra: (a) 1,2-bImb and its complexes **2** and **3** in CD_3CN; (b) 1,2-bImb and its complexes **1** and **3** in DMSO-d_6.

Information. In CD_3CN, the signals of the protons from imidazole rings (H_1, H_2, and H_3) are shifted upfield while those of others (H_4, H_5, and H_6) downfield after coordination. This observation is obviously contrary to the normal expectation that the ligand proton resonances should be shifted downfield in general upon coordination, and the signals of the protons near the coordination sites should be shifted downfield more than those of others because of the inductive effect of the metal ions.[5a,23] The most probable reason for such conflicting shifts is that the major species in solution retains its structure as observed in the solid state; that is, the two imidazole rings are face-to-face-arranged with protons on each ring shielded by the neighboring ring, resulting in an upfield shift due to the ring current effect. Such upfield shifts have been widely used to investigate aromatic π stacking in solution and found to be concentration-dependent.[24] In contrast, the methylene and phenyl

(24) (a) Shetty, A. S.; Zhang, J.; Moore, J. S. *J. Am. Chem. Soc.* **1996**, *118*, 1019. (b) Mizutani, M.; Kubo, I.; Jitsukawa, K.; Masuda, H.; Einaga, H. *Inorg. Chem.* **1999**, *38*, 420. (c) Fischer, B. E.; Sigel, H. *J. Am. Chem. Soc.* **1980**, *102*, 2998. (d) Yamauchi, O.; Odani, A. *J. Am. Chem. Soc.* **1985**, *107*, 5938.

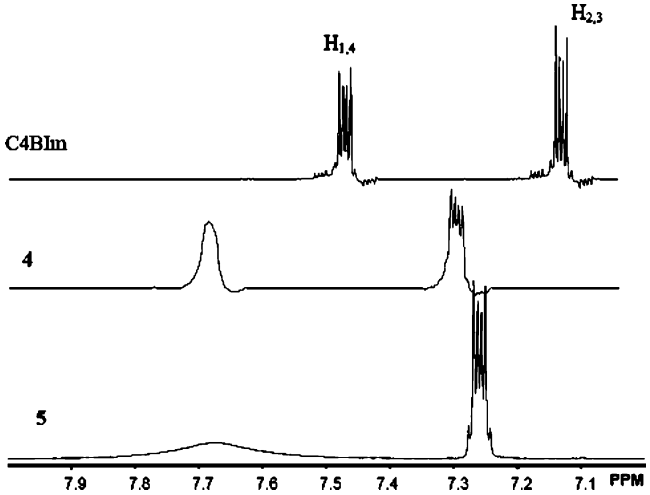

Figure 5. Partial ^{1}H NMR spectra for C4BIm and its complexes **4** and **5** in DMSO-d_6.

protons (H_4, H_5, and H_6) show the usual downfield shift, which is caused by the overall loss in electron density upon coordination. It is noticeable that different anions cause slightly different shifting values but do not alter the opposite shifting tendencies of two groups of signals, indicating that the same solution structures of the dimeric $[Ag_2L_2]^{2+}$ cations are formed with different counteranions. Similar proton shifts were observed by using DMSO-d_6 as the solvent. However, the shifts are not as significant as those in CD_3CN, suggesting that such proton shifts are also solvent-dependent.

Figure 5 shows the partial ^{1}H NMR spectra of C4BIm and its complexes recorded in DMSO-d_6 at ambient temperature. Unambiguous proton signal assignments were achieved by measuring and analyzing the 2D H,H−COSY spectrum of C4BIm, as depicted in Figure S7 in the Supporting Information. All protons experience a downfield shift upon coordination, indicating that no intramolecular aromatic π stacking is present and the dimeric $[Ag_2L_2]^{2+}$ cation may take the planar conformation as revealed in the solid-state structures. On the other hand, the signals of phenyl proton H_1 and H_4 resonances were significantly broadened, suggesting a dynamic process around this temperature, which will be discussed in detail later. Further verification of the dimeric structure comes from fast atom bombardment (FAB) mass spectra recorded for **4** and **5**. The peaks appearing at *m*/*z* 795, 505, and 397 are attributable to the $[Ag_2(C4BIm)_2\text{-}H]^+$, $[Ag_2(C4BIm)\text{-}H]^+$, and $[Ag(C4BIm)]^+$ species, respectively.

More detailed information on the solution structure can be convincingly obtained by ESI-MS. Figure 6 displays the ESI-MS spectra of complexes **3** and **5**, in which most of the salient peaks are assignable to potential coordination species in solution. Each species was verified by careful comparison of the isotopic patterns between the observed peak and the theoretical simulation, confirming the consistency of the molecular mass and the stoichiometric formulation. The ESI-MS spectrum of **3** recorded in acetonitrile shows peaks at *m*/*z* 804.9 (base peak), 585.1, 567.0, 387.9, and 347.3, evidently indicating the formation of coordination species $\{[Ag_2(1,2\text{-bImb})_2](CF_3CO_2)\}^+$, $[Ag(1,2\text{-bImb})_2]^+$, $\{[Ag_2(1,2\text{-}$

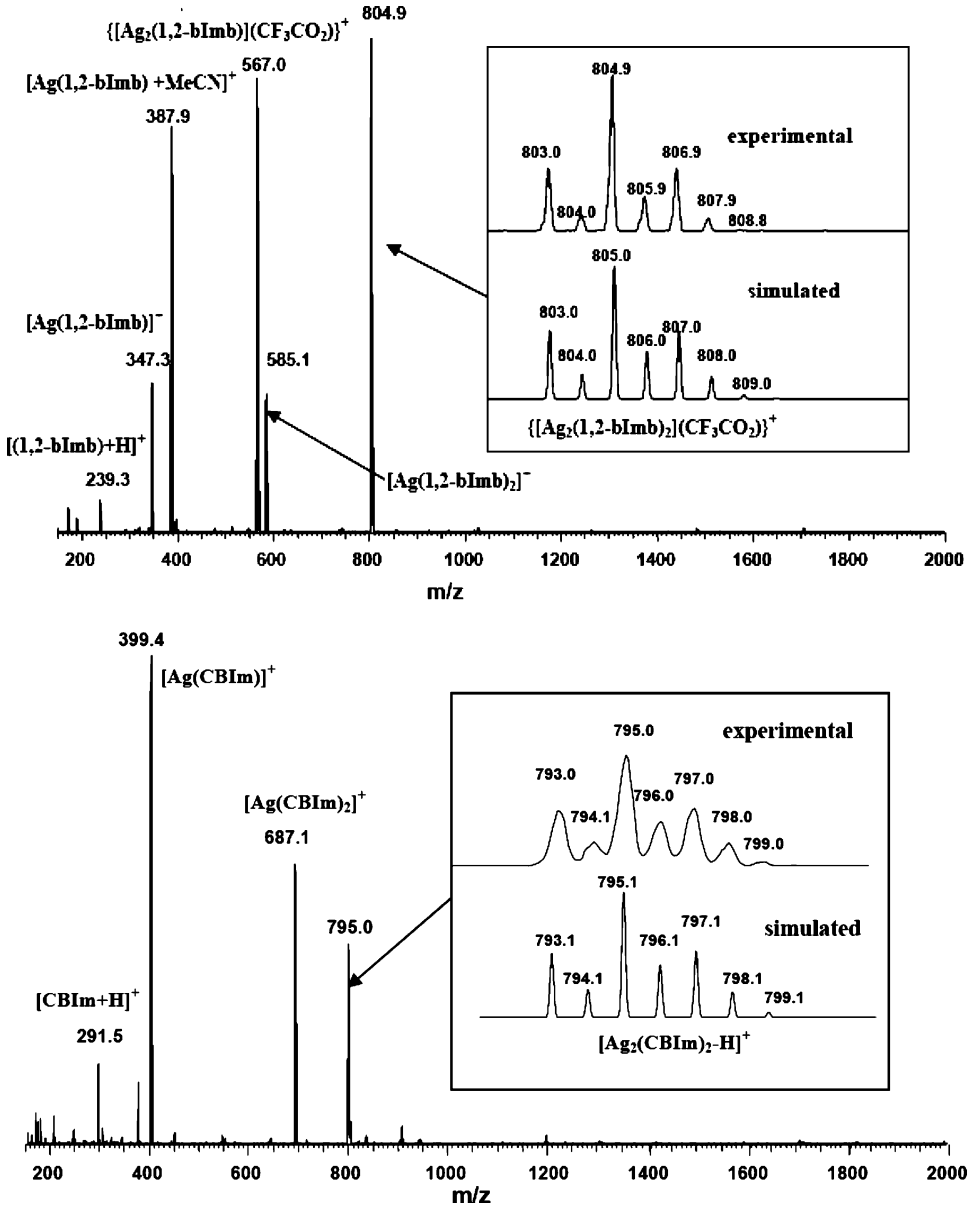

Figure 6. ESI-MS spectra of **3** (top) and **5** (bottom) in MeCN. Isotopic distribution of the selected peak is amplified with its simulation as the inset.

bImb)](CF_3CO_2)}$^+$, [Ag(1,2-bImb) + MeCN]$^+$, and [Ag(1,2-bImb)]$^+$, respectively. In addition to the dimeric cation $[Ag_2L_2]^{2+}$, there also exist the oligomeric species $[Ag_2L]^{2+}$, monomeric species $[AgL]^+$ and $[AgL_2]^+$, and solvated motif [AgL + MeCN]$^+$. These findings suggest that several solution species (or intermediates) simultaneously coexist, in agreement with what Lehn has termed "virtual combinatorial libraries", in which the prerequisite precursors will converge to the final product under normal circumstances.[25] The presence of the [AgL + MeCN]$^+$ motif may suggest that the dynamic equilibria among these species are established via a solvation-assisted dissociative pathway, as shown in Scheme 2.[14c,15] To further confirm this speculation, ESI-MS spectral measurements were carried out for complexes **1** and **2** in a MeCN/DMSO mixture. As expected, solution species attributable to $[Ag(1,2\text{-bImb})_2]^+$, [Ag(1,2-bImb) + MeCN]$^+$, [Ag(1,2-bImb) + DMSO]$^+$, and {$[Ag_2(1,2\text{-bImb})_2]$-$(ClO_4)$}$^+$ (for **1**) or {$[Ag_2(1,2\text{-bImb})_2](BF_4)$}$^+$ (for **2**) were clearly detected, as shown in Figure S8 in the Supporting Information. Similar equilibria may also exist for complex **5** in DMSO solution. The peaks appearing at *m*/*z* 795.0, 687.1, and 399.4 are attributed to $[Ag_2(C4BIm)_2\text{-H}]^+$, $[Ag(C4BIm)_2]^+$, and $[Ag(C4BIm)]^+$, respectively. Compared to those of **3**, the dimeric cation $[Ag_2L_2]^{2+}$ and monomeric species $[AgL_2]^+$ and $[AgL]^+$ are observed, but the oligomeric species $[Ag_2L]^{2+}$ and solvated motif are absent, although the former is detected by FAB-MS mentioned above. This again suggests that the solvent played an important role in solution dynamics and also affected ESI-MS measurement. Therefore, distribution of the species in solution was not estimated on the basis of the ESI-MS results. Alternatively, titration of a C4BIm solution with $AgCF_3CO_2$ monitored by in situ H^1 NMR was carried out.

(25) (a) Huc, I.; Lehn, M.-J. *Proc. Natl. Acad. Sci. U.S.A.* **1997**, *94*, 2106. (b) Lehn, J.-M.; Eliseev, A. V. *Science* **2001**, *291*, 2331.

Scheme 2 Potential Solution Dynamic Process for Complex **4** (or **5**)

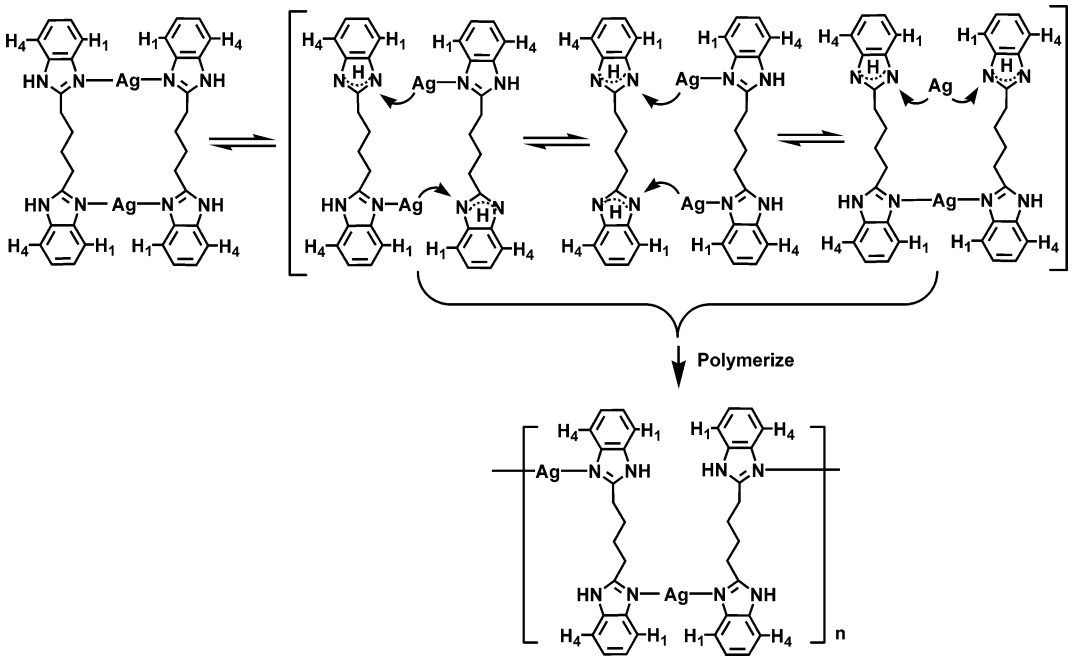

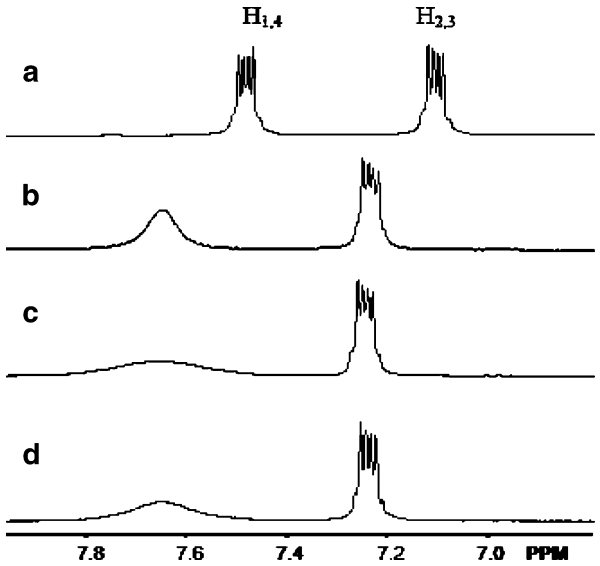

Figure 7. Titration of C4BIm with $AgCF_3CO_2$ in DMSO-d_6. Metal-to-ligand ratios: (a) 1:4; (b) 1:2; (c) 1:1; (d) 2:1.

As shown in Figure 7, when a small portion of silver(I) salt was added to the solution of the ligand (L:M > 4:1), the H^1 NMR spectrum essentially displayed the "free" ligand signal profile with a slight downfield shift. Continued addition of metal salts led to further downfield shift but not two separate sets of signals corresponding to the complex and the "free" ligand. In addition, the overlapped multiple signals of H_1 and H_4 started to broaden. These observations indicated complex formation, but the labile Ag−N bonds allowed rapid chemical exchange on the NMR time scale. The maximum signal shift and peak broadening was found for a 1:1 metal-to-ligand ratio, corresponding to quantitative formation of a disilver(I) metallacycle. Excess addition of metal salt showed little influence on chemical shifts but slightly sharpen the broadened peak. On the basis of these titration results, a combination of ESI-MS and solid-state structural information, it is rational to speculate that the disilver(I) cyclic $[Ag_2L_2]^{2+}$ motif is thermodynamically favored and predominant over other potential species in solution, consistent with the NMR and ESI-MS investigation results for complexes **1**−**3**.

The reason for H_1 and H_4 showing broadened resonances upon coordination can be easily explained by Scheme 2. In the absence of metal−ligand interaction, the amino proton moves rapidly between two tautomerized N atoms. Therefore, the phenyl protons H_1 and H_4 and the protons H_2 and H_3 are equivalent, giving rise to two sets of overlapping multiple signals. After coordination, the amino proton is fixed to one N atom so that the two N atoms become nonequivalent. This will make the adjacent H_1 and H_4 distinguishable, while the farside H_2 and H_3 are less affected, similar to the case of 2-substituted benzimidazole derivatives.[4] In other words, the signals of H_1 and H_4 resonances tend to separate while those of H_2 and H_3 still remain overlapped when Ag−ligand interactions happen. Because the Ag−N bond is labile in solution, such a separation of H_1 and H_4 signals will reflect the metal−ligand exchange, which can be monitored by VT-NMR once the dynamic process falls onto the NMR time scale. As a consequence, variable-temperature ^1H NMR was performed for complex **5** in DMF-d_7, which resembles polar solvent DMSO but has a lower freezing point, to elucidate the solution dynamics.

As shown in Figure 8, the spectrum of **5** in DMF-d_7 at 283 K exhibited the same broadened peak for H_1 and H_4 as that in DMSO-d_6. When the solution was cooled to 273 K, the broad signal was split into two separate peaks. At 223 K, two sharpened signals corresponding to well-resolved H_1 and H_4 appeared. This clearly indicated that the metal−ligand exchange slowed when the temperature was decreased. The coalescence temperature T_c was estimated at 278 K, and the exchange barriers $\Delta G^{\ddagger}$ (in kJ mol^{-1}) can be determined by

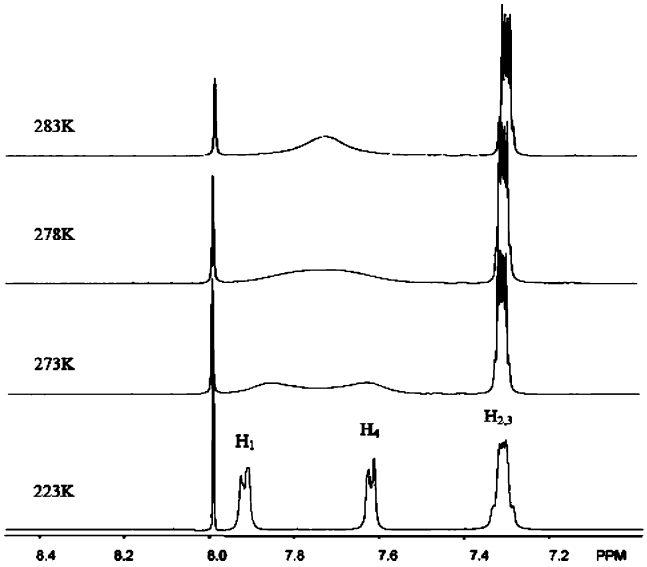

Figure 8. Temperature-dependent ^{1}H NMR spectra of complex **5** in DMF-d_7.

using the following Eyring equation (eq 1) together with equation 2,[26]

$$k = x\frac{k_B T}{h}e^{-\Delta G^{\ddagger}/RT} \quad (1)$$

$$\Delta G^{\ddagger} = 19.14T_c\left(10.32 + \log\frac{T_c}{k_c}\right) \times 10^{-3} \quad (2)$$

where x is the transmission coefficient (equal to 1), k_c is the exchange rate ($(\pi \times \Delta\upsilon)/\sqrt{2}$) at T_c, and $\Delta\upsilon$ the peak separation in the absence of exchange.

The calculated metal−ligand exchange barrier is 54.5 kJ mol^{-1} with the exchange rate 3.3×10^2 s^{-1}, which is comparable with the energy barrier 58.5 kJ mol^{-1} determined for the trinuclear silver(I) complex with thiazole N donors.[14a] Taking account of a few minor coordination motifs or intermediates in solution (vide ut supra), the energy barrier here may just represent the averaged free energy minimum for structural conversion between different solution species. On the other hand, because it is obvious that solvents play important roles in the proton chemical shifts and solution species formation as discussed above, the potential dynamic process may be considered to undergo a solvent-assisted dissociative exchanging mechanism (Scheme 2). Similar dynamic equilibria have been observed for other related systems.[14,15,22,27]

The activation energy estimated here suggests that the interaction between the Ag(I) ion and the N-donor ligand is comparable with that of strong hydrogen bonding.[28] Therefore, the structure of the final product can be easily influenced by various subtle factors such as the solvation effect, counterion interaction, and other supramolecular forces. This might partly account for why astonishingly diversified structures and topologies could be obtained from silver(I) and resembling ligands, giving rise to supramolecular isomerism. In the present instance, the dimeric $[Ag_2L_2]^{2+}$ motif represents the smallest cyclic entity in solution. Formation of open-ring oligomers is disfavored for enthalpic reasons, while larger macrocycles are disfavored because of entropic factors. However, on the basis of the equilibria among the dimeric cation and the potential oligomers and monomers, which may act as precursors, it is always possible for such precursors to polymerize, resulting in extended structures under appropriate conditions (Scheme 2). In other words, the energy barrier for the cyclic structure to convert into the extended structure should be comparable with subtle kinetic contributions upon crystallization. In this context, the polymeric structures are closely related to the cyclic ones. Solution dynamic investigation of the cyclic structure may be helpful to elucidate the assembly mechanisms for the polymeric isomers because the coordination polymers are known to show sparing solubility in most cases.[2c,9]

Counteranion Effect. It is known that the counteranions often play important roles to affect the assembly process of Ag(I) coordination polymers, leading to diversified network topologies due to the unique shape, size, and coordination ability of the anions.[28] The template effect and influence on the shape and size of the Ag(I) metallacycles have also been reported.[7] In the present cases, the counteranions weakly interact with the disilver(I) metallacycles, either through Ag···O and Ag···F secondary bonding (**1**−**3**) or through O−H···O and N−H···O hydrogen bonding (**4** and **5**), slightly tuning the shapes of the metallacycles, but do not significantly influence their formation. Altering the anions from noncoordinating BF_4^- or ClO_4^- to weakly coordinating $CF_3CO_2^-$ does not make a remarkable difference, indicating that the shape and size of the disilver(I) macrocycles depend mainly on the ligands rather than the counteranions. This is contrary to the findings of the disilver(I) macrocycles formed by the N-methylated bis(amidopyridine) ligand[7b] but consistent with our previous results.[29b] On the other hand, the crystal packing was found to be significantly influenced by the counteranions through the formation of distinguished supramolecular forces. As discussed in the Crystal Packing section, because the ligand 1,2-bImb has no NH hydrogen donor groups, all of the anions choose to interact with the Ag(I) ions and leave the ligand alone to form $\pi\cdots\pi$ interactions in **1**−**3**. The use of the spherical ClO_4^- and BF_4^- anions leads to the formation of similar 2D brick wall layers in **1** and **2**, whereas the use of the linear $CF_3CO_2^-$ anion results in cocrystallization of a methanol molecule to give rise to a 1D chain in **3**. By contrast, the presence of NH

(26) Friebolin, H. *Basic One- and Two-Dimensional NMR Spectroscopy*; Wiley-VCH: Weinheim, Germany, 1991; p 263.
(27) (a) Baxter, P. N. W.; Lehn, J.-M.; Rissanen, K. *Chem. Commun.* **1997**, 1323. (b) Xu, J.; Parac, T. N.; Raymond, K. N. *Angew. Chem., Int. Ed.* **1999**, *38*, 2878.
(28) (a) Khlobystov, A. N.; Blake, A. J.; Champness, N. R.; Lemenovskii, D. A.; Majouga, A. G.; Zyk, N. V.; Schröder, M. *Coord. Chem. Rev.* **2001**, *222*, 155. (b) Blake, A. J.; Champness, N. R.; Hubberstey, P.; Li, W.-S.; Withersby, A.; Schröder, M. *Coord. Chem. Rev.* **1999**, *183*, 117.
(29) (a) Chen, C.-L.; Su, C.-Y.; Xu, A.-W.; Zhang, H.-X.; Feng, X.-L.; Kang, B.-S. *Acta Crystallogr.* **2002**, *E58*, 916. (b) Tan, H.-Y.; Zhang, H.-X.; Ou, H.-D.; Kang, B.-S. *Inorg. Chim. Acta* **2004**, *357*, 869. (c) van Albada, G. A.; Lakin, M. T.; Veldman, N.; Spek, A. L.; Reedijk, J. *Inorg. Chem.* **1995**, *34*, 4910. (d) van Albada, G. A.; Veldman, N.; Spek, A. L.; Reedijk, J. *J. Chem. Crystallogr.* **2000**, *30*, 69.

Table 1. Crystallographic Data for Complexes **1**−**5**

formula	$C_{28}H_{28}Ag_2Cl_2N_8O_8$	$C_{28}H_{28}Ag_2B_2F_{82}N_8$	$C_{34}H_{36}Ag_2F_6N_8O_6$	$C_{42}H_{50}Ag_2Cl_2N_{10}O_{10}$	$C_{40}H_{40}Ag_2F_6N_8O_6$
M_w	891.22	865.94	982.45	1141.56	1058.54
crystal system	triclinic	triclinic	triclinic	triclinic	triclinic
space group	$P\bar{1}$	$P\bar{1}$	$P\bar{1}$	$P\bar{1}$	$P\bar{1}$
a/Å	8.184(2)	7.999(4)	9.418(2)	7.397(4)	9.450(5)
b/Å	8.478(2)	8.397(4)	10.244(3)	11.331(6)	10.407(5)
c/Å	12.504(3)	12.717(6)	11.219(3)	14.200(8)	11.061(6)
α/deg	99.007(3)	100.271(6)	69.045(3)	92.149(9)	101.076(9)
β/deg	92.494(4)	91.555(6)	88.145(4)	93.439(9)	98.593(9)
γ/deg	110.729(4)	110.988(5)	74.178(4)	107.522(9)	94.408(9)
V/Å^3	796.8(4)	780.8(6)	970.0(4)	1131.0(10)	1049.3(9)
Z	1	1	1	1	1
D_c/(g cm^{-3})	1.857	1.842	1.682	1.676	1.675
μ/mm^{-1}	1.460	1.337	1.092	1.053	1.016
R1	0.0425	0.0348	0.0447	0.0364	0.0397
wR2	0.1041	0.0955	0.1087	0.1206	0.1304

groups in the ligand C4BIm facilitates the formation of N−H···O hydrogen bonds; therefore, both ClO_4^- and $CF_3CO_2^-$ anions choose to interact with the ligand rather than the Ag(I) ions in **4** and **5**. The crystal packing is directed via a synergistic effect involving $\pi\cdots\pi$ stacking and hydrogen bonding. In **4**, a DMF molecule is incorporated in the crystal lattice by use of ClO_4^- and a 2D brick layer is formed, while in **5,** a water molecule participates in crystallization by use of $CF_3CO_2^-$ and a 3D framework is generated in comparison to the 2D layer in **4**.

Conclusion

Five new silver(I) complexes have been prepared in which the dimeric cations $[Ag_2L_2]^{2+}$ are exclusively formed, indicating that the semirigid 1,2-bImb bearing a xylylene spacer or the flexible C4BIm bearing an aliphatic $(CH_2)_4$ spacer can both be utilized to construct rectangular metallacycles. The solution structures explored by means of ^{1}H NMR and ESI-MS suggested that the predominant species in solution are consistent with the solid-state structures. The solution dynamics information obtained from NMR titration and VT-NMR measurement indicated that dynamic equilibria are established among a dimeric cation and other potential oligomers and monomers via a solvent-assisted dissociative exchange mechanism. The metal−ligand exchange barrier is estimated to be comparable with the energy of a strong hydrogen bond, which may partly account for the fact that formation of silver(I) complexes can be easily affected by various subtle factors to lead to supramolecular isomerism.

Experimental Section

All chemicals were of reagent grade from commercial sources and used without further purification. Elemental analyses were taken on a Perkin-Elmer 240 elemental analyzer. IR spectra were recorded on a Bruker EQUINOX55 FT-IR spectrophotometer using KBr disks in the 4000−400-cm^{-1} regions. ^{1}H NMR measurements were carried out on an INOVA 500NB spectrometer or a Mercury-Plus 300 spectrometer with $SiMe_4$ as the internal standard. FAB mass spectra were recorded on a VG ZAB-Hs instrument. ESI-MS was performed on a Thermo Finigan LCQDECA XP ion trap mass spectrometer or a LCMS-2010A liquid chromatograph/mass spectrometer. The accelerating cone voltage was set as low as possible to minimize the fragmentation process.

Safety Note*! Although we have not encountered any trouble with the silver perchlorate, it should be handled with appropriate precautions because perchlorate salts are known for their potential hazards.*

Preparation. The ligands 1,2-bImb and C4BIm were prepared according to the literature methods.[29] Complexes **1**−**5** were prepared in a similar manner. A CH_3CN solution of the silver salt AgX [0.10 mmol; X = ClO_4^- (**1** and **4**), $CF_3CO_2^-$ (**3** and **5**), BF_4^- (**2**)] was added dropwise to a stirred CH_3OH solution of 1,2-bImb·$2H_2O$ (0.027 g, 0.10 mmol) at room temperature for **1**−**3**. For complex **4** or **5**, C4BIm (0.029 g, 0.10 mmol) was used, and the reaction media were DMF/EtOH (1:1, v/v) for **4** and EtOH for **5**. The resulting mixture was continuously stirred for 10 min and then filtered. Colorless single crystals of **1**−**5** suitable for single-crystal X-ray diffraction analyses were obtained by slow diffusion of Et_2O into the clear reaction filtrate.

$[Ag_2(1,2\text{-bImb})_2](ClO_4)_2$ (1). Yield: 65%. Elem anal. Calcd (%) for $C_{28}H_{28}Ag_2Cl_2N_8O_8$: C, 37.74; H, 3.17; N, 12.57. Found: C, 38.09; H, 3.19; N, 12.87. ^{1}H NMR (DMSO-d_6, 25 °C): δ 7.55 (dd, 4H; H_5), 7.52 (dd, 4H; H_6), 7.41 (s, 2H; H_1), 7.14 (d, 2H; H_2), 6.94 (d, 2H; H_3), 5.42 (s, 4H; H_4). IR (KBr): ν 3132 (w), 3060 (w), 2936 (w), 1626 (w), 1516 (m), 1454 (w), 1386 (w), 1355 (m), 1299 (m), 1239 (m), 1113 (s), 1085 (s), 1030 (m), 949 (w), 831 (m), 789 (w), 734 (m), 654 (m), 623 (m) cm^{-1}.

$[Ag_2(1,2\text{-bImb})_2](BF_4)_2$ (2). Yield: 80%. Elem anal. Calcd (%) for $C_{28}H_{28}Ag_2B_2F_8N_8$: C, 38.84; H, 3.26; N, 12.94. Found: C, 39.03; H, 2.94; N, 13.05. IR (KBr): ν 3138 (m), 3055 (w), 2935 (w), 1623 (w), 1517 (m), 1458 (w), 1404 (w), 1343 (w), 1301 (m), 1241 (m), 1113 (s), 1076 (s), 1031 (s), 949 (w), 860 (w), 831 (m), 793 (w), 761 (m), 734 (m), 713 (m), 653 (m), 619 (m) cm^{-1}.

$[Ag_2(1,2\text{-bImb})_2](CF_3CO_2)_2\cdot 2CH_3OH$ (3·2CH_3OH). Yield: 35%. Elem anal. Calcd (%) for $C_{34}H_{36}Ag_2F_6N_8O_6$: C, 41.57; H, 3.69; N, 11.41. Found: C, 41.61; H, 3.50; N, 11.51. ^{1}H NMR (DMSO-d_6, 25 °C): δ 7.53 (s, 2H; H_1), 7.49 (m, 8H; $H_{5,6}$), 7.15 (d, 2H; H_2), 6.96 (d, 2H; H_3), 5.39 (s, 4H; H_4). IR (KBr): ν 3144 (w), 3112 (w), 3063 (w), 2957 (w), 1685 (m), 1574 (m), 1514 (s), 1459 (m), 1401 (m), 1356 (w), 1345 (w), 1286 (m), 1235 (m), 1110 (m), 1083 (m), 1028 (m), 932 (w), 837 (m), 747 (m), 718 (m), 659 (s), 622 (s) cm^{-1}.

$[Ag_2(C4BIm)_2](ClO_4)_2\cdot 2DMF$ (4·2DMF). Yield: 60%. Elem anal. Calcd (%) for $C_{21}H_{25}AgClN_5O_5$: C, 44.19; H, 4.41; N, 12.27. Found: C, 44.20; H, 4.37; N, 12.25. ^{1}H NMR (DMSO-d_6, 25 °C): δ 7.70 (b, 4H; $H_{1,4}$), 7.26 (m, 4H; $H_{2,3}$), 3.09 (t, 4H, −CCH_2CH_2−), 1.93 (m, 4H, −CCH_2CH_2−). IR (KBr): ν 3280 (s, br), 3061 (w), 2926 (w), 2858 (w), 1659 (s), 1624 (m), 1597 (m), 1535 (m), 1489 (w), 1454 (s), 1426 (m), 1382 (m), 1316 (m), 1280 (m), 1223 (m), 1089 (s), 1047 (m), 1003 (m), 929 (w), 847 (w), 747 (m), 668

(m), 621 (m), 436 (w) cm^{-1}. FAB-MS: *m*/*z* 795 $[Ag_2(C4BIm)_2\text{-}H]^+$, 505 $[Ag_2(C4BIm)\text{-}H]^+$, 397 $[Ag(C4BIm)]^+$.

$[Ag_2(C4BIm)_2](CF_3CO_2)_2\cdot 2H_2O$ (5·2H$_2$O). Yield: 63%. Elem anal. Calcd (%) for $C_{40}H_{40}Ag_2F_6N_8O_6$: C, 45.39; H, 3.81; N, 10.59. Found: C, 45.48; H, 3.78; N, 10.63. ^{1}H NMR (DMSO-d_6): δ 7.67 (b, 4H; $H_{1,4}$), 7.26 (m, 4H; $H_{2,3}$), 3.08 (t, 4H, $-CCH_2CH_2-$), 1.92 (m, 4H, $-CCH_2CH_2-$). IR (KBr): ν 3450−3310 (s, br), 3029 (w), 2957 (w), 2913 (w), 1674 (s), 1625 (m), 1535 (m), 1485 (w), 1454 (s), 1421 (m), 1345 (w), 1316 (w), 1281 (m), 1202 (s), 1045 (w), 1003 (w), 921 (w), 824 (m), 798 (m), 744 (s), 718 (m), 629 (w), 591 (w), 518 (w), 434 (w) cm^{-1}. FAB-MS: *m*/*z* 795 $[Ag_2(C4BIm)_2\text{-}H]^+$, 505 $[Ag_2(C4BIm)\text{-}H]^+$, 397 $[Ag(C4BIm)]^+$.

X-ray Crystallography. Experimental details of the X-ray analysis as well as the crystallographic data are listed in Table 1. Selected bond distances and bond angles are listed in Table 2. All diffraction data were collected on a Bruker Smart 1000 CCD diffractometer with graphite-monochromated Mo Kα radiation (λ = 0.710 73 Å) at room temperature using the program SMART[30] and processed by SAINT+.[31] Absorption corrections were applied using the SADABS program.[32] Space groups were determined from systematic absences and further justified by the results of the refinements. In all cases, the structures were solved by direct methods and refined using the full-matrix least-squares method against F^2 using SHELXTL software.[33] The coordinates of the non-hydrogen atoms were refined anisotropically. All hydrogen atoms were introduced in calculated positions and refined with fixed geometry with respect to their carrier atoms except for the hydrogen atoms of the CH_3OH for **2**, H21 in **4**, and H1WA and H1WB in **5**, which were located from difference syntheses and refined isotropically. F1 and F1′ atoms of anion BF_4^- in **3** are disordered and located at two positions, with an occupancy of 0.5 for each.

Table 2. Selected Bond Distances (Å) and Angles (deg) for Complexes **1**−**5**[a]

	Complex **1**		
Ag−N(1)	2.109(4)	Ag−N(3)#1	2.116(4)
N(1)−Ag−N(3)#1	174.3(2)		
	Complex **2**		
Ag−N(1)	2.099(3)	Ag−N(3)#1	2.098(3)
N(3)#1−Ag−N(1)	174.7 (1)	174.7 (1)	174.7 (1)
	Complex **3**		
Ag−N(1)#1	2.124(4)	Ag−N(3)	2.126(4)
N(1)#1−Ag−N(3)	168.2 (1)		
	Complex **4**		
Ag−N(1)	2.094(3)	Ag−N(3)#1	2.099(3)
N(1)−Ag−N(3)#1	170.1(1)		
	Complex **5**		
Ag−N(1)	2.076(3)	Ag−N(4)#1	2.088(3)
N(1)−Ag−N(4)#1	176.3(1)		

[a] Symmetry transformations used to generate equivalent atoms. **1**−**3**: #1, $-x+1, -y+2, -z+1$. **4**: #1, $-x+1, -y+1, -z+2$. **5**: #1, $-x, -y, -z$.

Acknowledgment. This work was supported by NNSF of China (Grant 20303027), NSF of Guangdong Province (Grant 04205405), and the Program for New Century Excellent Talents in University of China.

Supporting Information Available: Crystallographic data in CIF format, figures showing $\pi\cdots\pi$ interactions, hydrogen bonds, and crystal packing in **1**−**5**. This material is available free of charge via the Internet at http://pubs.acs.org.

IC050673O

(30) Bruker AXS. *SMART*, version 5.0; Bruker AXS: Madison, WI, 1998.
(31) Bruker AXS. *SAINT+*, version 6.0; Bruker AXS: Madison, WI, 1999.
(32) Blessing, R. *Acta Crystallogr., Sect. A* **1995**, *51*, 33.
(33) Sheldrick, G. M. *SHELX 97, Program for Crystal Structure Solution and Refinement*; Göttingen University: Göttingen, Germany, 1997.